PERGAMON

www.elsevier.nl/locate/poly

Polyhedron 20 (2001) 297–305

POLYHEDRON

Equilibrium studies on the protonation and Cu(II) complexation by an hexaaza macrocycle containing *p*-xylyl spacers. The crystal structure of the hexaprotonated ligand and the kinetics of decomposition of the Cu(II) complexes

Manuel G. Basallote [a,*], Joaquín Durán [a], María J. Fernández-Trujillo [a], M. Angeles Máñez [a], Miguel Quirós [b], Juan M. Salas [b]

[a] *Departamento de Ciencia de los Materiales e Ingeniería Metalúrgica y Química Inorgánica, Facultad de Ciencias, Universidad de Cádiz, Apartado 40, Puerto Real, 11510 Cádiz, Spain*

[b] *Departamento de Química Inorgánica, Facultad de Ciencias, Universidad de Granada, 18071 Granada, Spain*

Received 7 August 2000; accepted 30 October 2000

Abstract

The protonation constants of the ligand 3,6,9,16,19,22-hexaazatricyclo[22.2.2.2^{11,14}]triaconta-1(26),11(12),13,24,27, 29-hexaene (L, BPXD) have been determined in water at 25°C by potentiometric procedures and indicate a lower basicity than that corresponding to the analogue ligand with *m*-xylyl spacers between the diethylenetriamine subunits (BMXD). The crystal structure of a salt of H_6L^{6+} containing Br^- and NO_3^- as anions has been solved by X-ray diffraction procedures and reveals that the macrocycle adopts an almost planar configuration. The protonated amine groups are involved in a complex network of hydrogen bonds with the anions and water molecules, with two anions being placed close to the cavity of the macrocycle. Despite the lower basicity of BPXD, the stability of the mononuclear CuL^{2+} and $HCuL^{3+}$ complexes is several log units higher than that corresponding to the analogous BMXD complexes, which suggests the possibility of a different coordination mode for both closely related ligands. Actually, the whole set of stability constants for the mono and binuclear Cu(II)–L complexes can be rationalised by considering that the macrocycle acts as tetradentate in the mononuclear species. In contrast, the kinetic parameters for decomposition of the mono and binuclear Cu(II)–L complexes in acid solutions are only slightly different from those previously determined for the BMXD complexes. © 2001 Elsevier Science B.V. All rights reserved.

Keywords: Stability; Equilibrium constants; Macrocycle; Copper; Kinetics

1. Introduction

Symmetrical polyaza macrocycles of large size can coordinate simultaneously two metal ions and force them to be placed close to each other. As the donor atoms of the macrocycle usually do not complete the coordination spheres about the metal centres, the resulting binuclear complexes can interact with additional species, which often leads to the formation of bridged structures [1,2]. The special characteristics conferred to these complexes by the binuclear macrocycles can be used for recognition and catalytic purposes [3]. One special class of these macrocycles is that derived from reduction of the Schiff bases resulting from condensation of two diethylenetriamine (dien) molecules and different aldehydes (Chart 1). In addition to the possibility of formation of metal complexes, these ligands become highly protonated in acidic media and can form supramolecular species with different anions; the stability of these species depends largely on the charge and molecular structure of the anion, which can be also helpful for molecular recognition [4–8].

---

* Corresponding author. Tel.: +34-956-016-339; fax: +34-956-016-288.

E-mail address: manuel.basallote@uca.es (M.G. Basallote).

PII: S0277-5387(00)00630-6

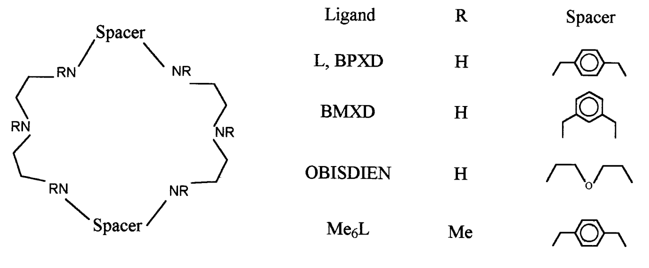

We are currently examining the possibility of special kinetic effects associated to the proximity of the metal centres in these complexes and have shown that the rate of coordination and release of two Cu(II) ions to BMXD and its related cryptand are very similar and occur with statistically controlled kinetics [9–11]. Macrocycles as BMXD that incorporate aromatic rings as an integral part of the major cycle are called cyclophanes and there are many comments in the recent literature about the effect of the aromatic rings on the properties of their metal complexes [12–14]. For this reason, we considered of interest to examine any possible change in the kinetics of reaction caused by a simple change of the *m*-xylyl groups in BMXD to *p*-xylyl in BPXD. The results are presented in this paper and show that the differences in the kinetic of decomposition of Cu(II) complexes with both cyclophanes are not large; however, there is an important difference of stability between the mononuclear complexes formed by both ligands.

2. Experimental

The ligand 3,6,9,16,19,22-hexaazatricyclo-[22.2.2.2^{11,14}]triaconta-1(26),11(12),13,24,27, 29-hexaene (L, BPXD) was prepared using the literature procedure [15] and was recrystallised from concentrated HBr. The positions of the signals in the ^{1}H NMR spectrum (D_2O solution) coincide with those previously reported [15] whereas the $^{13}C\{^1H\}$ NMR spectrum shows signals at 41.8, 43.8, 50.9, 131.3 and 131.5 ppm versus TMS consistent with the molecular structure. Potentiometric titrations of the sample used for the equilibrium and kinetic work lead to an experimental molecular weight of 871 ± 10 and a HBr–L ratio of 5.62 ± 0.06 (mean values and standard deviations from four titrations); so, it can be formulated as L.5.62 HBr (theor. mol. weight of 862). Crystals suitable for X-ray work were obtained by recrystallisation of this sample in 0.01 M HNO_3. The elemental analysis of the recrystallised sample (experimental: %C = 32.46, %H = 6.32, %N = 16.71) agrees well with the composition $C_{24}H_{38}N_6\cdot 1.33HBr\cdot 4.66HNO_3\cdot 4H_2O$ derived during the crystal structure determination (calculated: %C = 32.58, %H = 5.88, %N = 16.89).

The other reagents (diethylenetriamine, terephthaldicarboxaldehide, $NaBH_4$, KOH, KNO_3, KCl and $Cu(NO_3)_2\cdot 2.5H_2O$) were obtained from Aldrich and used without further purification. The solvents (acetonitrile and D_2O) were obtained from SDS. The NMR spectra were obtained with a Varian Unity 400 spectrometer and the elemental analysis was carried out at the Servicios Centralizados de Instrumentación Científica (Universidad de Granada).

2.1. Crystal structure determination

An irregularly shaped crystal, dimensions $0.45 \times 0.4 \times 0.35$ mm^3, was mounted on a Siemens P4 diffractometer with Mo Kα radiation for X-ray work at room temperature. The unit cell was determined from 39 randomly oriented reflections in the range $5 < \Theta < 18°$. A total of 6791 reflections, averaged to 5719 independent ones were measured in the range $2 < \Theta$ 30°, $-1 \le h \le 11$, $-14 \le k \le 14$, $-16 \le l \le 16$. Data were corrected for Lorentz, polarisation and empirically (ω-scans) for absorption (transmission range, 0.5062–0.4796).

The structure was solved by direct methods and refined by full-matrix least squares on F^2 using the software package SHELXS-97 [16]. The most intense diffraction feature was initially assigned to a bromide ion, but subsequent refinement was not satisfactory, intense holes appearing near this atom in the ΔF maps, as well as three peaks around it forming an equilateral triangle. According to this, the supposition was made that the bromide ion had not full occupancy of the site, which should be completed by nitrate ions; after some trial and error, occupancy of 2/3 was set for the bromide and 1/3 for the nitrate. The nitrogen atom of this nitrate ion is clouded by the bromide and it was artificially introduced at the geometrical centre of the three peaks assigned to the oxygen atoms and N–O distances were fixed to 1.24 Å. With this disordered scheme, the refinement improved appreciably and peaks and holes in the ΔF maps fell below 1 e Å^{-3}. The resulting formulation fits better with the elemental analysis than those implying full occupancy of the bromide ions.

All non-hydrogen atoms were refined anisotropically except those belonging to the partial occupancy nitrate. Hydrogen atoms of the organic ligand were introduced in their ideal positions, the presence of two hydrogen atoms on each nitrogen atom being confirmed by the H-bond scheme. Hydrogen atoms of water molecules were located in the ΔF maps and refined with fixed O–H (0.86 Å) and H–H (1.35 Å) distances.

2.2. Equilibrium measurements

Potentiometric titrations were carried out at $25.0 \pm 0.1°C$ under a N_2 atmosphere in the presence of 0.10 M supporting electrolyte (KNO_3 or KCl). The titrations were carried out with a Crison 2002 pH-meter provided with an Ingold combined electrode. The system was calibrated to read pH as $-\log[H^+]$ by fitting the data corresponding to the titration of a HNO_3 solution with KOH. Stock solutions of KOH and $Cu(NO_3)_2 \cdot 2.5H_2O$ were prepared and titrated with potassium hydrogen phthalate (phenolphthalein indicator) and EDTA (murexide indicator), respectively. Solutions of the ligand (50.0 cm^3) with an initial concentration close to 2×10^{-3} M were prepared in water containing the supporting electrolyte, and the required amount of Cu(II) solution was then added before titration with KOH.

For every one of the supporting electrolytes used (KNO_3 and KCl) two titrations of the ligand were initially carried out and used to obtain the protonation constants of the ligand and the actual molecular weight of the sample. Reported values of the protonation constant correspond to the mean value and standard deviation of both measurements. The equilibrium constants for the formation of Cu(II)–L complexes were then obtained from three titrations of solutions containing Cu(II) and L in 2:1, 1:1 and 0.5:1 molar ratios. In all cases titrations had to be interrupted at relatively low pH because of precipitation, which precludes the determination of the formation constants of the hydroxocomplexes and leads to larger uncertainties in the value of $\log \beta_{CuL}$ (see Section 3). The reported values of the equilibrium constants correspond now to the mean values and standard deviations of the values derived from the three titrations.

The analysis of the titration data was carried out with program BEST and the species distribution curves were obtained with programs SPE and SPEPLOT [17]. The number of points measured was different for every titration and ranges from 59 to 63 for titrations of the ligand alone and from 36 to 45 for titrations of Cu(II)–L mixtures. The range of pH covered expands from ca. 2.7 to 10.5 for titrations of the ligand alone and from 2.7 to 4.4, 4.5 or 7.7 for titrations of solutions containing Cu(II) and L at 2:1, 1:1 and 0.5:1 ratios, respectively. During all refinements the value of $\log K_w$ was fixed at -13.78. For titrations containing Cu(II) and L, the formation constants corresponding to the different protonated forms of the ligand were fixed at the values derived from titrations of the ligand alone, and Cu(II)–OH^- complexes were also introduced in the model with formation constants fixed at their corresponding literature values [18].

2.3. Kinetic experiments

The dissociation kinetics of Cu(II)–L complexes were carried out at 25.0 ± 0.1°C using an Applied Photophysics SX17MV stopped-flow instrument. The ligand concentration in the solutions used in the kinetic work were calculated using the experimental molecular weight of 871, and then the required amount of titrated Cu(II) solution was added to achieve the desired Cu(II):L molar ratio. In this way, two solutions with 0.5:1 and 2:1 ratios (Cu(II):L) were prepared and the pH was then adjusted to values that favour the formation of the mono (0.5:1 solution) or the binuclear (2:1 solution) complexes. The resulting solutions were mixed in the stopped flow instrument with solutions of HNO_3 of different concentrations. All experiments were carried out under pseudo-first-order conditions (acid excess) with the ionic strength of all the solutions adjusted to 0.10 M with KNO_3. The wavelength was selected at 280 nm from preliminary experiments that were also used to confirm the independence of the rate constants with respect to the concentration of complex. The kinetic traces could be always well fitted by a single exponential using the standard software of the instrument, and reported values correspond to the mean of six measurements, the standard deviation being always lower than 5%.

Table 1
Logarithms of the protonation constants at 25°C for macrocycle L and related compounds [a]

K	Equilibrium quotient	L (KNO_3) [b]	L (KCl) [b]	BMXD (KNO_3) [c]	BMXD (KCl) [d]	Me_6L (NaCl) [e]
K_{HL}	[HL]/[L][H]	9.52 ± 0.04	9.54 ± 0.03	9.54	9.51	8.93
K_{H_2L}	$[H_2L]/[HL][H]$	8.57 ± 0.02	8.76 ± 0.04	8.76	8.77	8.22
K_{H_3L}	$[H_3L]/[H_2L][H]$	7.96 ± 0.01	8.16 ± 0.02	8.05	7.97	7.35
K_{H_4L}	$[H_4L]/[H_3L][H]$	7.06 ± 0.05	7.26 ± 0.04	7.32	7.09	6.44
K_{H_5L}	$[H_5L]/[H_4L][H]$	3.2 ± 0.2	3.3 ± 0.1	3.67	3.79	1.5
K_{H_6L}	$[H_6L]/[H_5L][H]$		2.5 ± 0.2	3.41	3.27	

[a] The charges have been omitted for clarity and the nature of the supporting electrolyte is indicated in parentheses. The concentration of supporting electrolyte is 0.10 M in all cases except for Me_6L (0.15 M of NaCl).

[b] This work.

[c] Mean values from Refs. [9,19].

[d] Ref. [5].

[e] Ref. [12].

Table 2
Summary of crystal data collection and refinement parameters for $(H_6L)Br_{1.33}(NO_3)_{4.66}{\cdot}4H_2O$

Empirical formula	$C_{24}H_{52}Br_{1.33}N_{10.67}O_{18}$
Formula weight	884.64
Wavelength (Å)	0.71073
Crystal system	triclinic
Space group	$P\bar{1}$
Unit cell dimensions	
a (Å)	8.4812(13)
b (Å)	10.5077(12)
c (Å)	11.8177(13)
α (°)	80.425(9)
β (°)	71.135(10)
γ (°)	86.857(11)
V (Å^3)	982.7(2)
Z	1
D_{calc} (mg m^{-3})	1.495
Absorption coefficient (mm^{-1})	1.469
F(000)	461
Crystal size (mm)	$0.45 \times 0.4 \times 0.35$
θ Range for data collection (°)	1.84–30.00
Limiting indices	$-1 \leq h \leq 11$, $-14 \leq k \leq 14$, $-16 \leq l \leq 16$
Reflections collected/unique	6791/5719 [$R_{int} = 0.0688$]
Completeness to $\theta = 30.00$	99.7%
Absorption correction	empirical
Max./min. transmission	0.5062 and 0.4796
Refinement method	full-matrix least-squares on F^2
Weighting scheme	$w = 1/[\sigma^2(F_o^2)+(0.2P)^2]$ where $P = (F_o^2+2F_c^2)/3$
Data/restraints/parameters	5719/9/262
Goodness-of-fit on F^2	1.116
Final R indices $[I > 2\sigma(I)]$	$R_1 = 0.0724$, $wR_2 = 0.2408$
R indices (all data)	$R_1 = 0.1297$, $wR_2 = 0.3170$
Largest difference peak and hole (e Å^{-3})	0.675 and -0.733

3. Results and discussion

3.1. Equilibrium studies on ligand protonation

The equilibrium constants for protonation of L are included in Table 1, which also contains some literature data [5,9,12,19] for comparative purposes. We initially carried out the titrations in the presence of KNO_3 as supporting electrolyte and were surprised to find that only five constants corresponding to the formation of H_xL^{x+} up to $x = 5$ could be obtained. The introduction of the H_6L^{6+} species in the equilibrium model does not lead to any improvement in the quality of the fit, which suggests that the log K value for its formation from H_5L^{5+} must be lower than ca. 2.5. While the first four constants are not very different from those found for BMXD, the analogous ligand with m-xylyl spacers (Table 1), the value of $\log K_{H_5L}$ is unusually low and also indicates a decreased basicity of the central nitrogens on every dien subunit. Titration of the ligand in the presence of KCl as supporting electrolyte confirmed these results, although a value of 2.5 could be obtained in this case for $\log K_{H_6L}$ (see Table 1). Except for $\log K_{HL}$, the values in KCl are 0.2 units higher than in KNO_3, which suggests that $\log K_{H_6L}$ in KNO_3 is probably close to 2.3. Table 1 also contains literature data for Me_6L that indicate that the presence of methyl substituents on the amine groups cause an almost constant decrease of 0.5–0.6 log units in the first four protonation constants. However, the value of $\log K_{H_5L}$ for the methylated macrocycle is only 1.5 and no value was reported for the sixth protonation step; extrapolation of these values to the unsubstituted L leads to estimations not very different from our experimental values. Thus, the data are consistent with those previously reported and confirm that a change from m- to p-xylyl spacers does not change the basicity of the terminal NH groups but causes a significant decrease in the basicity of the central amine groups in every dien subunit.

As the effect of the change in the aromatic ring is mainly observed on the basicity of the central amine groups and these groups appear to be very far from the rings for the effect to have a direct electronic or steric origin, an alternative explanation is required. An unusual decrease in the basicity of some of the amine groups has been also observed for cyclam and other macrocycles, and several possible explanations have been proposed [13,20]. One of the possibilities is that formation of intramolecular hydrogen bonds between protonated and unprotonated donor groups gives a special stability to some partially protonated forms of the ligand, thus making more difficult the subsequent protonation steps. Interestingly, the crystal structure of the tetraprotonated perchlorate salt of Me_6L shows intramolecular hydrogen bonds between the protonated terminal ammonium groups and the unprotonated central amine groups in every dien subunit [12]. We tried to confirm this observation by obtaining the structure of a H_4L^{4+} salt but the isolated crystals contained the hexaprotonated ion, whose structure is described in the next section. However, the close similarity between the L and Me_6L macrocycles makes reasonable the assumption that the reduced basicity of the central amine groups in both ligands with respect to BMXD is the consequence of a higher flexibility of the macrocycle that allows a conformation suitable for intramolecular hydrogen bonding.

3.2. The crystal structure of $(H_6L)Br_{1.33}(NO_3)_{4.66}{\cdot}4H_2O$

The structure of a salt of the hexaprotonated macrocycle H_6L^{6+} containing bromide and nitrate as counter-anions has been solved by X-ray diffraction methods, and a summary of crystal data collection and refinement is given in Table 2. The apparently complex formula of the salt is simply the consequence of the existence of a certain disorder between the anion positions that does not preclude an accurate determination of the structure of the cation. The macrocycle adopts an almost planar structure with the two phenyl rings being almost parallel to each other and perpendicular to the plane of the macrocycle (Fig. 1). The shape of the cavity is close to a rectangle whose dimensions can be estimated by measuring the distance between equivalent carbons in both phenyls (mean value of 10.0 Å) and the distance from each atom in one dien subunit to the average plane of the other subunit (mean value of 4.4 Å). The same quasi-planar configuration of the macrocycle has been found for related ligands containing two dien subunits and different spacers [5,6]. All the bond distances and angles within the protonated macrocycle can be considered normal and selected values are included in Table 3 together with the distances of the hydrogen bonds in the structure.

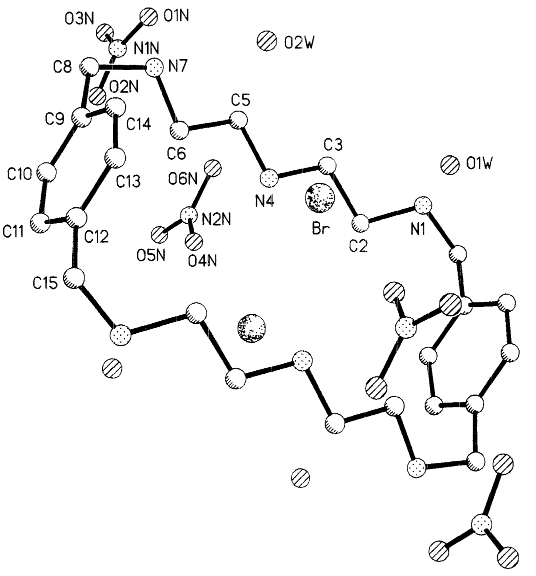

Fig. 1. Ball and stick plot of the $(H_6L)Br_{1.33}(NO_3)_{4.66}\cdot4H_2O$ salt with labelling scheme.

Table 3
Selected bond lengths (Å), bond angles (°) and hydrogen bonds (Å) for $(H_6L)Br_{1.33}(NO_3)_{4.66}\cdot4H_2O$ [a]

N(1)–C(15) # 1	1.491(5)	N(1)–C(2)	1.517(5)
C(2)–C(3)	1.511(6)	C(3)–N(4)	1.491(5)
N(4)–C(5)	1.484(5)	C(5)–C(6)	1.530(5)
C(6)–N(7)	1.482(5)	N(7)–C(8)	1.501(5)
C(8)–C(9)	1.497(5)	C(9)–C(10)	1.364(5)
C(9)–C(14)	1.403(5)	C(10)–C(11)	1.387(5)
C(11)–C(12)	1.387(5)	C(12)–C(13)	1.395(5)
C(12)–C(15)	1.508(5)	C(13)–C(14)	1.398(5)
C(15) # 1–N(1)–C(2)	114.0(3)	C(3)–C(2)–N(1)	107.7(3)
N(4)–C(3)–C(2)	111.3(3)	C(5)–N(4)–C(3)	109.9(3)
N(4)–C(5)–C(6)	110.4(3)	N(7)–C(6)–C(5)	108.0(3)
C(6)–N(7)–C(8)	115.1(3)	C(9)–C(8)–N(7)	112.8(3)
C(10)–C(9)–C(14)	118.7(3)	C(10)–C(9)–C(8)	121.9(4)
C(14)–C(9)–C(8)	119.4(3)	C(9)–C(10)–C(11)	121.9(4)
C(10)–C(11)–C(12)	119.5(3)	C(11)–C(12)–C(13)	120.0(3)
C(11)–C(12)–C(15)	119.5(3)	C(13)–C(12)–C(15)	120.5(3)
C(12)–C(13)–C(1)	119.3(3)	C(13)–C(14)–C(9)	120.5(3)
N(1) # 1–C(15)–C(12)	111.8(3)		
Hydrogen bonds			
N(1)···O(5N) # 2	2.789(4)	N(1)···O(1W)	2.804(5)
N(4)···O(4N)	2.762(5)	N(4)···Br	3.440(3)
N(4)···O(8N)	2.827(12)	N(7)···O(1N)	2.848(4)
N(7)···O(2W)	2.879(5)	O(1W)···Br	3.460(4)
O(1W)···O(8N)	2.777(13)	O(1W)···O(3N) # 3	2.793(6)
O(2W)···Br # 4	3.556(5)	O(2W)···O(9N) # 4	2.705(15)
O(2W)···Br	3.364(5)	O(2W)···O(8N)	2.856(13)

[a] Symmetry transformations used to generate equivalent atoms: # 1 $-x+1$, $y+1$, $-z+1$; # 2 $-x+2$, $-y+1$, $-z$; # 3 $-x+1$, $-y+1$, $-z$; # 4 $-x$, $-y+1$, $-z+1$.

The NO_3^- and Br^- anions reside outside the cavity of the macrocycle, although they are placed close to it and interact with the ammonium groups through a complex network of hydrogen bonds. Two of the four nitrates not involved in disorder are hydrogen-bonded to a terminal NH_2^+ group and to a water molecule, the latter being also connected to a bromide and to an adjacent H_6L^{6+} cation. The other two non-disordered nitrates are hydrogen-bonded to one of the central NH_2^+ groups and to a terminal NH_2^+ in another molecule. The remaining anion positions are disordered with an occupancy factor of 2/3 for Br^- and 1/3 for NO_3^-, although for simplicity only the bromides have been considered in the comments, figures and tables. Both bromides are placed one at each side of the plane defined by the macrocycle and interact exclusively with one of the dien subunits of the molecule (Fig. 1). Every bromide has direct hydrogen bonds to the central NH_2^+ group and two water molecules, the latter molecules being also connected to a terminal NH_2^+ group. The bromides also participate in the intermolecular interactions by forming another hydrogen bond with one of the water molecules associated to an adjacent H_6L^{6+} ion. This rather complicated pattern of hydrogen bonds can be summarised in the following four types, where the subscripts t and c indicate terminal and central, and the superscripts A and B refer to different H_6L^{6+} ions:

$$(NH_2^+)_t^A\text{-----}(H_2O)\text{-----}(Br^-)\text{-----}(NH_2^+)_c^A$$

$$(NH_2^+)_t^A\text{-----}(NO_3^-)\text{-----}(H_2O)\text{-----}(NH_2^+)_t^B$$

$$(NH_2^+)_t^A\text{-----}(NO_3^-)\text{-----}(NH_2^+)_c^B$$

$$(NH_2^+)_c^A\text{-----}(Br^-)\text{-----}(H_2O)\text{-----}(NH_2^+)_t^B$$

In recent years there is great interest in the possibility of encapsulating simple inorganic anions as NO_3^- or Br^- inside the cavity of protonated polyaza macrocyclic compounds. Encapsulation of an anion requires it to be placed inside the cavity with formation of several hydrogen bonds with the ammonium groups of the same molecule; these multiple interactions lead to a high stability constant of the resulting supramolecular species, which can be useful for recognition purposes.

Table 4
Equilibrium data for the formation of Cu(II)–L complexes at 25°C and 0.10 M of supporting electrolyte (KNO_3 or KCl), and comparison with literature values for related systems [a]

log β [b]				L = BPXD		L = BMXD		L = OBISDIEN		L = Me_6BPXD
				Log *K*		Log *K*		Log *K*		Log *K*
Species	KNO_3	KCl	*K*	KNO_3	KCl	KNO_3 [c]	KCl [d]	KNO_3 [e]	KCl [f]	NaCl [g]
CuL	17.50 [h]	18.41 [h]	[CuL]/[Cu][L]	17.50	18.41	13.82	13.63	16.46	16.21	10.03
HCuL	24.97 ± 0.22	26.24 ± 0.11	[HCuL]/[CuL][H]	7.47	7.83	8.47	8.40	8.01	7.81	7.93
H_2CuL	29.36 ± 0.05	30.41 ± 0.06	[H_2CuL]/[HCuL][H]	4.39	4.17	7.48	7.20	7.46	7.76	6.77
Cu_2L	24.12 ± 0.18	25.98 ± 0.11	[Cu_2L]/[CuL][Cu]	6.62	7.57	9.94	10.86	10.84	10.79	8.32

[a] The charges have been omitted for clarity.

[b] Reported values correspond to the mean and standard deviation of three determinations from solutions containing Cu(II) and L in 2:1, 1:1 and 0.5:1 molar ratios.

[c] Mean values from Refs. [9,19].

[d] Ref. [22].

[e] Ref. [1].

[f] Ref. [21].

[g] Ref. [23] (0.15 M NaCl).

[h] An estimation of the error is not given because this species could only be detected in the titration of solutions containing Cu(II) and L in 0.5:1 molar ratios. As this species never represents more than 10–20% of the total concentration of ligand, the error in the reported value is significantly higher than for the other log β values.

Although there are previous reports showing the encapsulation of one nitrate by the tetra-protonated form of the macrocyle O-BISDIEN [7] and of two nitrates by the hexa-protonated form of a related cryptand [8], most crystal structures of this kind of compound show the anions residing outside the cavity. An intermediate situation is that in which the anions are oriented towards the centre of the cavity and forced to be placed close to the plane of the macrocycle as a consequence of the formation of two (or more) hydrogen bonds with ammonium groups within the same molecule. In the case of BMXD·6HBr, two bromides are hydrogen-bonded simultaneously to a central and a terminal NH_2^+ group and they are displaced from the plane of the macrocycle by only 1.6 Å, which has been considered a particular case of quasi-encapsulation [5]. A quite similar situation is found in the present work for the bromides in $(H_6L)Br_{1.33}(NO_3)_{4.66}\cdot 4H_2O$, although in this case one of the two hydrogen bonds to the same H_6L^{6+} ion is mediated by a water molecule and the distance to the least-squares plane of the six nitrogen atoms in the macrocycle is 1.75 Å. In any case, the differences found between the hydrogen-bonding networks for L and closely related compounds indicates that the positions of the anions are determined mainly by the crystal packing forces and so, they can not be considered representative of the structure in solution. Moreover, depending on the pH, the solutions contain different protonated forms of the macrocycles and every one of these forms will show its own behaviour towards anions.

3.3. Equilibrium studies on the formation of Cu(II)–L complexes

The stability constants derived for the formation of mono and binuclear Cu(II) complexes of L both in KNO_3 and KCl media are included in Table 4, which also includes literature data for related ligands [1,9,19,21–23]. Because of precipitation at relatively low pH during the titrations, no information could be obtained about the formation of Cu(II)–L–hydroxo complexes. For the same reason, the log K_{CuL} values for the formation of the CuL complex had to be derived exclusively from the last points of titrations of solutions containing 0.5 equiv. of Cu(II) per equiv. of L and so, they are affected by errors larger than usual. However, log β_{HCuL} is well defined in the whole set of titration data and log K_{HCuL} for protonation of CuL in this kind of ligand is always ca. 8, which confirms the validity of the log K_{CuL} values in Table 4. Thus, despite the lower overall basicity of the macrocycle with *p*-xylyl spacers, formation of the mononuclear complex occurs with log K_{CuL} higher than 17 in both media, several log units more stable than the corresponding complex of the analogous macrocycle with *m*-xylyl spacers. To our knowledge, these values represent the highest formation constant for CuL^{2+} complexes with macrocycles containing two dien subunits separated by rigid spacers and, actually, they are even higher than log K_{CuL} for diethylenetriamine (15.9) [18].

The equilibrium constant in Table 4 for conversion of CuL^{2+} to the protonated $HCuL^{3+}$ species is somewhat smaller than for related ligands, but it can be considered almost normal. However, further protonation to form the diprotonated species occurs with $\log K_{H_2CuL}$ values that are only slightly higher than 4, three log units smaller than for related ligands (Table 4). An unusually low value of $\log K_{Cu_2L}$ close to 7 is also observed for conversion of CuL^{2+} to Cu_2L^{4+}, in such a way that the values of $\log \beta_{Cu_2L}$ become comparable to those found for the complexes with related ligands.

The set of stability constants in Table 4 for the formation of the mono and binuclear Cu(II)–L complexes can not be rationalised with the conventional equilibrium model that has been applied successfully to most metal complexes of related symmetrical binucleating macrocycles. According to this model [24] formation of the mononuclear complex should occur through coordination of the metal ion to the three nitrogens in one dien subunit, which would result in $\log K_{CuL}$ values slightly smaller than for Cu(II)–dien because of the decreased basicity of the amine groups in the macrocycles. As the CuL^{2+} complex would contain an uncoordinated dien subunit, protonation to form H_xCuL complexes should occur with $\log K$ values close to the corresponding protonation constants of the free ligand, with small differences caused by the different electrostatic repulsion with the metal ion. On the other hand, conversion of CuL^{2+} to Cu_2L^{4+} should occur through coordination of the second ion to the uncoordinated subunit, with an equilibrium constant smaller than $\log K_{CuL}$ as a consequence of the proximity of both metal centres. As pointed out above, this model requires some modification to account for the equilibrium data corresponding to BPXD. The nature of the macrocycle and the proximity of $\log \beta_{Cu_2L}$ to the values found for related ligands suggests that the binuclear complex adopts the usual structure with a Cu(II) coordinated to every dien subunit, as confirmed by the crystal structures of two isomers of $[Cu_2(BPXD)(CH_3COO)_2(H_2O)_2](ClO_4)_2$ [25]. However, the values of $\log K_{CuL}$ higher than usual and close to those found for complexes with tetraaza macrocycles strongly suggest that the metal ion in the mononuclear complex is coordinated to four amine groups in the macrocycle. As a consequence of the closer proximity of the metal centre to the uncoordinated amine groups, protonation to $HCuL^{3+}$ is then expected to occur with a formation constant slightly smaller than for other complexes, although the $\log \beta$ value is still high and suggests that the tetradentate behaviour of L is probably maintained in $HCuL^{3+}$. Further protonation to H_2CuL^{4+} or coordination of a second ion to form Cu_2L^{4+} require the breaking of a Cu–N bond, which would explain the unusually low tendency of CuL^{2+} to form these species. A similar explanation was offered years ago to account for the high stability of the CuL^{2+} complex of OBISDIEN [1], but in that case the $\log K$ values for conversion to $HCuL^{3+}$, H_2CuL^{4+} and Cu_2L^{4+} are normal (Table 4) and do not provide additional evidence for a tetradentate behaviour of the ligand. Although the stability data can be rationalised in terms of tetradentate behaviour of the ligand in the CuL^{2+} and $HCuL^{3+}$ complexes, alternative explanations can not be ruled out. Thus, any structural feature as an special arrangement of the amine groups or an interaction between parallel phenyl rings can also lead to an increased stability of these species and, consequently, to a satisfactory explanation of the experimental results.

The present equilibrium results indicate that a subtle change from the *m*- to *p*-xylyl spacers is enough to cause a large stability difference between the CuL^{2+} complexes of the closely related BMXD and BPXD macrocycles. Again, it is unlikely that the difference has an electronic origin because in that case BPXD should be more basic than BMXD and the experimental evidence indicate just the opposite. Thus, it appears that the high stability of the mononuclear BPXD complex must be associated to a higher flexibility of the macrocyclic ring that allows a conformation suitable for tetracoodination, a conclusion similar to that previously achieved from the ligand protonation data. In contrast, the stability of the Cu(II) complexes with Me_6L can be interpreted according to the conventional equilibrium model, which indicates that methylation of the amine groups leads to a decreased flexibility of the macrocycle that makes it unable to act as tetradentate.

3.4. Acid assisted dissociation kinetics of Cu(II)–L complexes

The existence of a large number of Cu(II)–L complexes in solution hinders the kinetic analysis of their reactions, but we have shown previously that interesting conclusions about the relative rates of decomposition of the mono and the binuclear complexes can be obtained by selecting suitable starting conditions [9–11,26]. The species distribution curves for solutions containing Cu(II) and L at 0.5:1 and 2:1 molar ratios are included in Fig. 2 as a function of pH. These curves show that the only complexes in 0.5:1 solutions at pH close to 5 are mononuclear, whereas the binuclear complex represents more than 80% of the total species in the 2:1 solutions at pH close to 6. Under these conditions, addition of an excess of acid in a stopped-flow instrument allows the kinetic study of the decomposition processes corresponding to both complexes (Eqs. (1) and (2)). In all cases, the initial absorbance coincides with that corresponding to the starting complex (no reaction within the stopped-flow mixing time) and kinetic traces can be fitted by a single exponential; the results so obtained are included in Table 5. In both cases, the observed rate constants show a clear tendency to saturation (Fig. 3) and can be fitted by Eq. (3)

with $a = 54 \pm 3$ s^{-1} and $b = 88 \pm 13$ M^{-1} (mononuclear complex) or $a = 43 \pm 2$ s^{-1} and $b = 57 \pm 6$ M^{-1} (binuclear complex), where a and b have the same meaning than for related complexes [10]. No attempt was made to obtain kinetic data for the decomposition of the unprotonated CuL^{2+} complex because this species only represents a small fraction of the total complex in solution under conditions that avoid precipitation.

$$H_xCuL^{(2+x)+} + H^+ \rightarrow Cu^{2+} + H_zL^{z+} \tag{1}$$

$$Cu_2L^{4+} + H^+ \rightarrow 2Cu^{2+} + H_zL^{z+} \tag{2}$$

$$k_{obs} = \frac{ab[H^+]}{1 + b[H^+]} \tag{3}$$

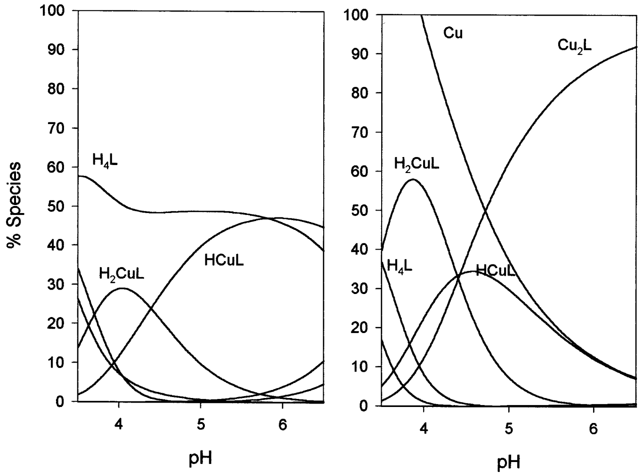

Fig. 2. Species distribution curves for solutions containing Cu(II) and L at 0.5:1 (left) and 2:1 (right) molar ratios. The percentages are relative to the total concentration of ligand, which was set at the value used in the kinetic experiments. Only the major components have been labelled.

Table 5
Observed rate constants for the decomposition of the mono and binuclear complexes of Cu(II) with BPXD at 25°C and 0.10 M KNO_3

[HNO_3] (M)	k_{obs} (s^{-1})	
	Mononuclear [a]	Binuclear [b]
2.62×10^{-3}	9.66	4.92
5.24×10^{-3}	19.25	10.96
1.05×10^{-2}	24.96	16.13
1.57×10^{-2}	29.64	20.14
2.10×10^{-2}	34.60	22.96
4.19×10^{-2}	43.07	30.71

[a] The starting solution of the complex contained Cu(II) and L in 0.5:1 molar ratio ($[L]_0 = 2 \times [Cu]_0 = 3.98 \times 10^{-4}$ M) and the pH was then adjusted to 5.06.

[b] The starting solution of the complex contained Cu(II) and L in 2:1 molar ratio ($[L]_0 = 0.5 \times [Cu]_0 = 3.98 \times 10^{-4}$ M) and the pH was then adjusted to 5.87.

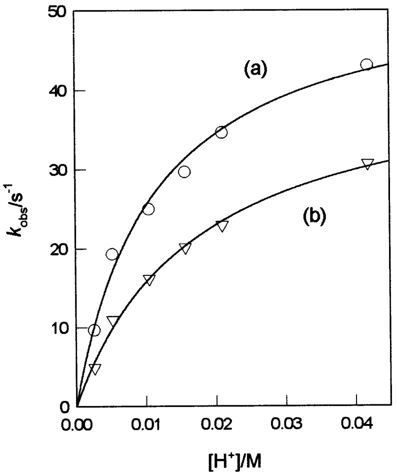

Fig. 3. Plots of k_{obs} vs. the acid concentration for the decomposition of the mononuclear (a) and binuclear (b) Cu(II)–L complexes.

At a glance, kinetic data appear to indicate that the binuclear complex decomposes at a slightly lower rate than the mononuclear one. However, we have shown [10,11] that the rate of release of both metal ions in this type of complexes is statistically controlled and that the lower rate for the binuclear complexes is simply a consequence of the simplification of the rate law to a single exponential under certain mathematical conditions. If both metal centres behave as independent chromophores and the binuclear complexes decompose in two steps with rate constants $2 \times k_{obs}$ and k_{obs}, a single exponential with rate constant k_{obs} is measured experimentally. The kinetic data for the Cu(II)–L complexes are close to those found for the complexes with dien, BMXD and related ligands [11,27], which confirms that the rate of decomposition of the Cu(II)–polyamine complexes is essentially determined by the type of chelate rings in the complex. The major differences with respect to the decomposition of the analogous Cu(II)–BMXD complexes are the absence of an additional acid-independent term and changes of the a and b parameters by factors of ca. 2 and 20 [10]. However, these differences are similar to those recently found [11] between different species formed by Cu(II) with the same macrocycle (BMXD) and so, they can not be assigned to a different kinetic behaviour of the complexes formed by both macrocycles.

4. Supplementary data

Crystallographic data for the structural analysis have been deposited with the Cambridge Crystallographic Data Centre, CCDC no. 147762. Copies of this information may be obtained free of charge from The Director, CCDC, 12 Union Road, Cambridge, CB2

1EZ, UK (fax: + 44-1223-336033; e-mail: deposit@ccdc.cam.ac.uk or www: http://www.ccdc.cam.ac.uk).

Acknowledgements

Financial support by the Spanish Dirección General de Enseñanza Superior (Proyecto PB96-1516) and Junta de Andalucía (Grupos FQM-0137 and FQM-0195) is gratefully acknowledged.

References

[1] R.J. Motekaitis, A.E. Martell, J.P. Lecomte, J.M. Lehn, Inorg. Chem. 22 (1983) 609.

[2] P.K. Coughlin, J.C. Dewan, S.J. Lippard, E. Watanabe, J.M. Lehn, J. Am. Chem. Soc. 101 (1979) 265.

[3] (a) R.J. Motekaitis, A.E. Martell, Inorg. Chem. 30 (1991) 694. (b) Q. Lu, J.Reibenspies, A.E. Martell, R.J. Motekaitis, Inorg. Chem. 35 (1996) 2636. (c) M.T.B. Luiz, B. Szpoganicz, M. Rizzotto, A.E. Martell, M.G. Basallote, Inorg. Chim. Acta 254 (1997) 345. (d) K.P. McCue, D.A. Voss, Jr., C. Marks, J.R. Morrow, J. Chem. Soc., Dalton Trans. (1998) 2961. (e) M.T.B. Luiz, B. Szpoganicz, M. Rizzotto, M.G. Basallote, A.E. Martell, Inorg. Chim. Acta 287 (1999) 134.

[4] J. Cullinane, R.I. Gelb, T.N. Margulis, L.J. Zompa, J. Am. Chem. Soc. 104 (1982) 3048.

[5] D.A. Nation, J. Reibenspies, A.E. Martell, Inorg. Chem. 35 (1996) 4597.

[6] Q. Lu, R.J. Motekaitis, J. Reibenspies, A.E. Martell, Inorg. Chem. 34 (1995) 4958.

[7] G. Papoyan, K. Gu, J. Wiorkievicz-Kuczera, K. Kuczera, K. Bowman-James, J. Am. Chem. Soc. 118 (1996) 1354.

[8] S. Mason, T. Clifford, L. Seib, K. Kuczera, K. Bowman-James, J. Am. Chem. Soc. 120 (1998) 8899.

[9] M.G. Basallote, J. Durán, M.J. Fernández-Trujillo, M.A. Máñez, B. Szpoganicz, J. Chem. Soc., Dalton Trans. (1999) 1093.

[10] M.G. Basallote, J. Durán, M.J. Fernández-Trujillo, M.A. Máñez, J. Chem. Soc., Dalton Trans. (1999) 3817.

[11] M.G. Basallote, J. Durán, M.J. Fernández-Trujillo, M.A. Máñez, Polyhedron 20 (2001) 75.

[12] C. Bazzicalupi, A. Bencini, A. Bianchi, V. Fusi, C. Giorgi, P. Paoletti, A. Stefani, B. Valtancoli, J. Chem. Soc., Perkin Trans. 2 (1995) 275.

[13] A. Bencini, A. Bianchi, E. García-España, M. Micheloni, J.A. Ramírez, Coord. Chem. Rev. 188 (1999) 97.

[14] (a) M.B. Inoue, E.F. Velazquez, F. Medrano, K.L. Ochoa, J.C. Galvez, M. Inoue, Q. Fernando, Inorg. Chem. 37 (1998) 4070. (b) M.I. Burguete, P. Díaz, E. García-España, S.V. Luis, J.F. Miravet, M. Querol, J.A. Ramirez, J. Chem. Soc., Chem. Commun. (1999) 649.

[15] D. Chen, A.E. Martell, Tetrahedron 47 (1991) 6895.

[16] G.M. Sheldrick, Acta Crystallogr., Sect. A 46 (1990) 467.

[17] A.E. Martell, R.J. Motekaitis, Determination and Use of Stability Constants, VCH, New York, 1992.

[18] R.M. Smith, A.E. Martell, R.J. Motekaitis, NIST Critical Stability Constants of Metal Complexes Database, US Department of Commerce, Gaithesbourgh, 1993.

[19] R. Menif, A.E. Martell, P.J. Squattrito, A.E. Clearfield, Inorg. Chem. 29 (1990) 4723.

[20] A. Bianchi, M. Micheloni, P. Paoletti, Coord. Chem. Rev. 110 (1991) 17.

[21] P.E. Jurek, A.E. Martell, R.J. Motekaitis, R.D. Hancock, Inorg. Chem. 34 (1995) 1823.

[22] D.A. Nation, A.E. Martell, R.I. Carroll, A. Clearfield, Inorg. Chem. 35 (1996) 7246.

[23] C. Bazzicalupi, A. Bencini, A. Bianchi, V. Fusi, C. Giorgi, P. Paoletti, A. Stefani, B. Valtancoli, Inorg. Chem. 34 (1995) 552.

[24] M.G. Basallote, A.E. Martell, Inorg. Chem. 27 (1988) 4219.

[25] H.L. Zhu, L.M. Zheng, C.Y. Duan, X.Y. Huang, W.M. Bu, M.F. Wu, W.X. Tang, Polyhedron 17 (1998) 3909.

[26] M.J. Fernández-Trujillo, B. Szpoganicz, M.A. Máñez, L.T. Kist, M.G. Basallote, Polyhedron 15 (1996) 3511.

[27] S. Siddiqui, R.E. Shepherd, Inorg. Chem. 22 (1983) 3726.